All-optical light storage in bound states in the continuum and release by demand

E. N. Bulgakov, K. N. Pichugin, and A. F. Sadreev

L.V. Kirensky Institute of Physics, Academy of Sciences, 660036 Krasnoyarsk, Russia

*almas@tnp.krasn.ru

Abstract: In the framework of the temporal coupled mode theory we consider bound states embedded in the continuum (BSC) of photonic crystal waveguide as a capacity for light storage. A symmetry protected BSC occurs in two off-channel microresonators positioned symmetrically relative to the waveguide. We demonstrate that the symmetry protected BSC captures a fraction of a light pulse due to the Kerr effect as the pulse passes by the microresonators. However the amount of captured light is found to be strongly sensitive to the parameters of the gaussian light pulse such as basic frequency, duration and intensity. In contrast to the above case the BSC resulted from a full destructive interference of two eigenmodes of a single microresonator accumulates a fixed amount of light dependent on the material parameters of the microresonator but independent of the light pulse. The BSCs in the Fabry-Perot resonator show similar effects. We also show that the accumulated light can be released by a secondary pulse. These phenomena pave a way for all-optical storage and release of light.

References and links

1. T. F. Krauss, "Slow light in photonic crystal waveguides," J. Phys. D **40**, 2666–2670 (2007).
2. T. Baba, "Slow light in photonics crystals," Nat. Photonics, **2**, 465–473 (2008).
3. M. Notomi, "Manipulating light with strongly modulated photonic crystals," Rep. Progr. Phys. **73**, 096501 (2010).
4. A. Melloni, F. Morichetti, and M. Martinelli, "Optical slow wave structures," Opt. Photon. News **14**, 44–48 (2003).
5. F. Morichetti, C. Ferrari, A. Canciamilla, and A. Melloni, "The first decade of coupled resonator optical waveguides: bringing slow light to applications," Laser Photonics Rev. **6**, 74–96 (2012).
6. H. Gersen, T. J. Karle, R. J. P. Engelen, W. Bogaerts, J. P. Korterik, N. F. van Hulst, T. F. Krauss and L. Kuipers, "Real-space observation of ultraslow light in Photonic Crystal Waveguides," Phys. Rev. Lett. **94**, 073903 (2005).
7. I. V. Shadrivov, A. A. Sukhorukov, and Y. S. Kivshar, "Guided modes in negative-refractive-index waveguides," Phys. Rev. E **67**, 057602 (2003).
8. J. He, Y. Jin, Z. Hong, and S. He, "Slow light in a dielectric waveguide with negative-refractive-index photonic crystal cladding," Opt. Express , **16**, 11077–11082 (2008).
9. S. He, Y. He, and Y. Jin, "Revealing the truth about trapped rainbow storage of light in metamaterials," Sci. Rep. **583**, 1–9 (2012).
10. K. L. Tsakmakidis , A. D. Boardman, and O. Hess, "Trapped rainbow storage of light in metamaterials," Nature **450**, 397–401 (2007).
11. V. N. Smolyaninova, I. I. Smolyaninov, A. V. Kildishev, and V. M. Shalaev, "Experimental observation of the trapped rainbow," Appl. Phys. Lett. **96**, 211121 (2010).
12. R. Yang, W. Zhu, and J. Li, "Realization of trapped rainbow in 1D slab waveguide with surface dispersion engineering," Opt. Express **23**(5), 6326–6335 (2015).

13. S. Fan, P. R. Villeneuve, J. D. Joannopoulos, M. J. Khan, C. Manolatou, and H. A. Haus, "Theoretical analysis of channel drop tunneling processes," Phys. Rev. B **59**(24), 15882–15892 (1999).
14. S. P. Shipman and S. Venakides, "Resonant transmission near nonrobust periodic slab modes," Phys. Rev. E **71**, 026611 (2005).
15. D. C. Marinica, A. G. Borisov, and S. V. Shabanov, "Bound States in the Continuum in Photonics," Phys. Rev. Lett. **100**, 183902 (2008).
16. E. N. Bulgakov and A. F. Sadreev, "Bound states in the continuum in photonic waveguides inspired by defects," Phys. Rev. B **78**, 075105 (2008).
17. S. Longhi, "Transfer of light waves in optical waveguides via a continuum," Phys. Rev. A **78**, 013815 (2008).
18. S. Longhi, "Optical analogue of coherent population trapping via a continuum in optical waveguide arrays," J. Mod. Opt. **56**, 729–737 (2009).
19. F. Dreisow, A. Szameit, M. Heinrich, R. Keil, S. Nolte, A. Tünnermann, and S. Longhi, "Adiabatic transfer of light via a continuum in optical waveguides," Opt. Lett. **34**, 2405–2407 (2009).
20. Y. Plotnik, O. Peleg, F. Dreisow, M. Heinrich, S. Nolte, A. Szameit, and M. Segev, "Experimental observation of optical bound states in the continuum," Phys. Rev. Lett. **107**, 183901 (2011).
21. G. Corrielli, G. Della Valle, A. Crespi, R. Osellame, and S. Longhi, "Observation of surface states with algebraic localization," Phys. Rev. Lett. **111**, 220403 (2013).
22. S. Weimann, Y. Xu, R. Keil, A. E. Miroshnichenko, A. Tunnermann, S. Nolte, A. A. Sukhorukov, A. Szameit, and Yu. S. Kivshar, "Compact surface Fano states embedded in the continuum of waveguide arrays," Phys. Rev. Lett. **111**, 240403 (2013).
23. C. W. Hsu, B. Zhen, S.-L. Chua, S. G Johnson, J. D. Joannopoulos, and M. Soljačić, "Bloch surface eigenstates within the radiation continuum," Light: Sci. Appl. **2**, 1–5 (2013).
24. C. W. Hsu, B. Zhen, J. Lee, S.-L. Chua, S. G. Johnson, J. D. Joannopoulos, and M. Soljačić, "Observation of trapped light within the radiation continuum," Nature **499**, 188–191 (2013).
25. E. N. Bulgakov and A. F. Sadreev, "Robust bound state in the continuum in a nonlinear microcavity embedded in a photonic crystal waveguide," Opt. Lett. **39**(17), 5212–5215 (2014).
26. Y. Yang, C. Peng, Y. Liang, Z. Li, and S. Noda, "Analytical perspective for bound states in the continuum in photonic crystal slabs," Phys. Rev. Lett. **113**, 037401 (2014).
27. B. Zhen, C. W. Hsu, L. Lu, A. D. Stone, and M. Soljačić, "Topological nature of bound states in the radiation continuum," Phys. Rev. Lett. **113**, 257401 (2014).
28. E. N. Bulgakov and A. F. Sadreev, "Bloch bound states in the radiation continuum in a periodic array of dielectric rods," Phys. Rev. A **90**, 053801 (2014).
29. M. Song, H. Yu, C. Wang, N. Yao, M. Pu, J. Luo, Z. Zhang, and X. Luo, "Sharp Fano resonance induced by a single layer of nanorods with perturbed periodicity," Opt. Express **23**(3), 2895–2903 (2015).
30. M. Zhang and X. Zhang, "Ultrasensitive optical absorption in graphene based on bound states in the continuum," Sci. Rep. **5**, 8266 (2015).
31. E. N. Bulgakov and A. F. Sadreev, "Resonance induced by a bound state in the continuum in a two-level nonlinear Fano-Anderson model," Phys. Rev. B **80**, 115308 (2009);
32. E. N. Bulgakov and A. F. Sadreev, "Bound states in photonic Fabry-Perot resonator with nonlinear off-channel defects," Phys. Rev. B **81**, 115128 (2010).
33. M. I. Molina, A. E. Miroshnichenko, and Yu. S. Kivshar, "Surface bound states in the continuum," Phys. Rev. Lett. **108**, 070401 (2012).
34. E. N. Bulgakov, K. N. Pichugin, and A. F. Sadreev, "Symmetry breaking for transmission in a photonic waveguide coupled with two off-channel nonlinear defects," Phys. Rev. B **83**, 045109 (2011).
35. J. Joannopoulos, R. D. Meade, and J. Winn, *Photonic Crystals: Molding the Flow of Light* (Princeton University Press, 1995).
36. D. Englund, I. Fushman, and J. Vuckovic, "General recipe for designing photonic crystal cavities," Opt. Express **13**, 5961–5975 (2005).
37. M. Notomi, E. Kuramochi, and H. Taniyama, "Ultrahigh-Q nanocavity with 1D photonic gap," Opt. Express **16**, 11096–11102 (2009).
38. Sh. Fan, W. Suh, and J. D. Joannopoulos, "Temporal coupled-mode theory for the Fano resonance in optical resonators," J. Opt. Soc. Am. A **20**, 569–572 (2003).
39. W. Suh, Z. Wang, and S. Fan, "Temporal coupled-mode theory and the presence of non-orthogonal modes in lossless multimode cavities," IEEE J. Quantum Electron. **40**(10), 1511–1518 (2004).
40. E. N. Bulgakov and A. F. Sadreev, "All-optical diode based on dipole modes of Kerr microcavity in asymmetric L-shaped photonic crystal waveguide," Opt. Lett. **39**(7), 1787–1790 (2014).
41. K. Busch, S. F. Mingaleev, A. Garcia-Martin, M. Schillinger, and D. Hermann, "The Wannier function approach to photonic crystal circuits," J. Phys.: Cond. Mat. **15**, R1233–R1256 (2003).
42. K. N. Pichugin and A. F. Sadreev, "Frequency comb generation for wave transmission through the nonlinear dimer," J. Phys.: Conf. Ser. **574** 012037 (2015).
43. H. Friedrich and D. Wintgen, "Interfering resonances and bound states in the continuum," Phys. Rev. A **32**, 3231-3242 (1985).

44. A. E. Miroshnichenko, S. F. Mingaleev, S. Flach, and Yu. S. Kivshar, "Nonlinear Fano resonance and bistable wave transmission," Phys. Rev. E **71**, 036626 (2005).
45. Z. Wang and S. Fan, "Compact all-pass filters in photonic crystals as the building block for high-capacity optical delay lines," Phys. Rev. E **68**, 066616 (2003).

1. Introduction

One of the most technologically attractive approaches for light storage is the use of slow wave designs of optical periodic structures to slow down the light pulse [1–3]. Various methods and designs such as direct-coupled resonators [2, 4, 5] and photonic crystal (PhC) waveguides [6] have been proposed to slow down the group velocity of light. Slow light waveguides composed of left-handed materials have been also proposed [7, 8]. In these waveguides, the time average power in the left-handed material layer flows in an opposite direction of that in the normal dielectric layer. For the case when light flows are almost equal, slow light and even trapping can be achieved [9]. The frequency of the slow light regime varies with the thickness of the layer resulting in so-called trapped rainbow [10–12].

In this paper we propose to employ bound states in the continuum (BSC) as a novel capacity for light storage. Recently the BSCs have attracted much interest in photonics owing to a possibility to trap light in various photonic systems [13–30]. The BSC is a localized solution of the Maxwell equations with a discrete eigenfrequency coexisting with the extended modes of continuous spectrum of the PhC waveguide or radiation continuum. Our main goal is to demonstrate that the BSCs are able to capture light due the Kerr effect in the microresonators. Moreover we demonstrate that the application of a secondary light pulset releases trapped light making the BSC potentially interesting for all-optical light storage and release.

The physics of the light storage by the BSCs is the following. Assume for a moment that the amplitude of the injected wave is so small that we can neglect the nonlinearity. Because the BSC is completely decoupled from the continuum it can not be probed by the incoming wave. However with the increase of the injected power the Kerr effect of the microresonators becomes important killing two birds with one stone. First, there is no necessity for tuning material parameters because the Kerr effect in the microresonators results in occurrence of self-induced BSCs [31–33]. Second, the nonlinearity couples the BSC with the continuum so that the injected wave excites the BSC transforming it into a quasi-BSC. Once the pulse has passed by the microeresonator the quasi-BSC is again decoupled from the waveguide and becomes a true BSC. As a result some amount of light is trapped in the true BSC opening an opportunity for light storage. Finally, the application of a secondary pulse again transforms the true BSC into a quasi-BSC with finite life-time and releases the light with substantial or even 100% efficiency. Below we inspect these ideas on the basis of three simplest 2D PhC designs which realize the self-induced BSCs.

2. Symmetry protected BSC

We begin with the most obvious system in which light can be trapped by the symmetry protected BSC [16, 20, 23, 34]. For clear visualization of such a BSC we present in Fig. 1 2D photonic crystal (PhC) layout with electric field profile of the antisymmetric mode which is the BSC [16]. However interested reader can easily design different layouts based for instance on nano resonators with extremely high Q-factors in air-hole 2D PhC system [35–37]. In order to present the mechanism of light storage in the BSC in the most comprehensive form we assume that among all eigenmodes of the microresonator only the lowest monopole TM mode has the eigenfrequency ω_0 embedded into the first TM propagation band of the directional PhC waveguide. Then the eigenmodes of the total system of two resonators can be classified as symmetric
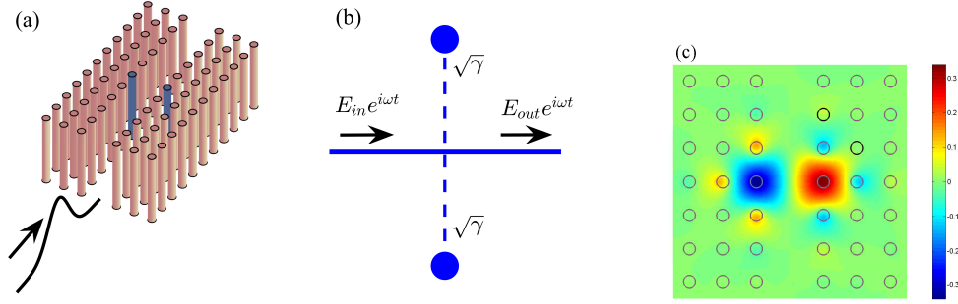
Fig. 1. (a). The single row of the rods is removed from the PhC to form a directional photonic waveguide which supports a band of guided even TM mode. Two defect rods shown in gray with the Kerr effect are inserted symmetrically relative to the waveguide to form identical off-channel optical microresonators coupled with the waveguide. (b). Equivalent CMT presentation for PhC layout. (c). Electric field profile in the symmetry protected BSC.

and antisymmetric modes

$$A_{s,a} = (A_1 \pm A_2)/2, \quad \omega_{s,a} = \omega_0 \pm u, \tag{1}$$

where variable $A_j, j = 1, 2$ presents the amplitude of the monopole mode in the j-th microresonator and u is due to overlapping of these modes. For simplicity we disregard the dispersion properties of the waveguide and consider that light with the amplitude E_{in} is injected into the waveguide as shown in equivalent coupled mode theory layout in Fig. 1(b). We assume the injected light is symmetrical relative to the cental line of the waveguide. Then the temporal coupled mode theory (CMT) equations have the following form [38, 39]

$$-i\dot{A}_s = (\omega_s + 2i\gamma)A_s - i\sqrt{\gamma}E_{in}e^{i\omega t},$$
$$-i\dot{A}_a = \omega_a A_a, \tag{2}$$

where the term $\sqrt{\gamma}$ is responsible for the coupling of the off-channel resonators with the waveguide. Thus, the temporal CMT equations clearly demonstrate that the antisymmetric mode A_a is a symmetry protected BSC.

If the waveguide can support only the symmetrical propagating mode then injected light can not probe the BSC. However that is true only for the linear case. If the microresonators are nonlinear owing to the Kerr effect there is a nonlinear shift of the eigenfrequency $\omega_0 \rightarrow \omega_0 + \lambda|A_j|^2$ where $|A_j|^2$ is the intensity of light in the j-th microresonator. Substituting Eq. (1) into the CMT equations (2) we obtained the CMT equations modified with account of the Kerr effect as follows

$$-i\dot{A}_1 = (\omega_0 + \lambda|A_1|^2)A_1 + i\gamma(A_1 + A_2) + uA_2 - i\sqrt{\gamma}E_{in}(t)e^{i\omega t},$$
$$-i\dot{A}_2 = (\omega_0 + \lambda|A_2|^2)A_2 + i\gamma(A_1 + A_2) + uA_1 - i\sqrt{\gamma}E_{in}(t)e^{i\omega t}, \tag{3}$$

where λ is the nonlinear coefficient [35, 40]

$$\lambda = \frac{\omega_0 n_0 c^2 n_2^2}{8\pi a^2} \int E_m^4(x,y)dxdy, \quad N_m = \int \varepsilon(x,y)E_m^2(x,y)dxdy = \frac{a^2}{cn_2} \tag{4}$$

with integration over the cross-section of the defect rod. $E_m(x,y)$ is the monopole eigenmode normalized via the constant N_m. The profile of the monopole mode is clearly seen in

the BSC mode formed by two defect rods shown in Fig. 1. We present estimations based on the PhC structure in Fig. 1(a) which consists of GaAs rods with $n_0 = 4.3, a = 0.5\mu m$, radius $0.18\mu m$. The single row of the rods is removed from the PhC to form a directional photonic waveguide which supports a band of guided even TM mode spanning from 0.302 to the upper band edge 0.444 [41]. Two nonlinear defect rods with the same radius $0.18\mu m, n_0 = 2$ and $n_2 = 2 \cdot 10^{-12}W/cm^2$ shown in gray are inserted symmetrically relative to the waveguide to form identical off-channel optical microresonators coupled with the waveguide. Estimations give the following values of the relevant parameters for the equivalent CMT layout: $\omega_0 = 0.352, \gamma \approx 0.01, u \approx 0.001, \lambda \approx 10^{-4}$.
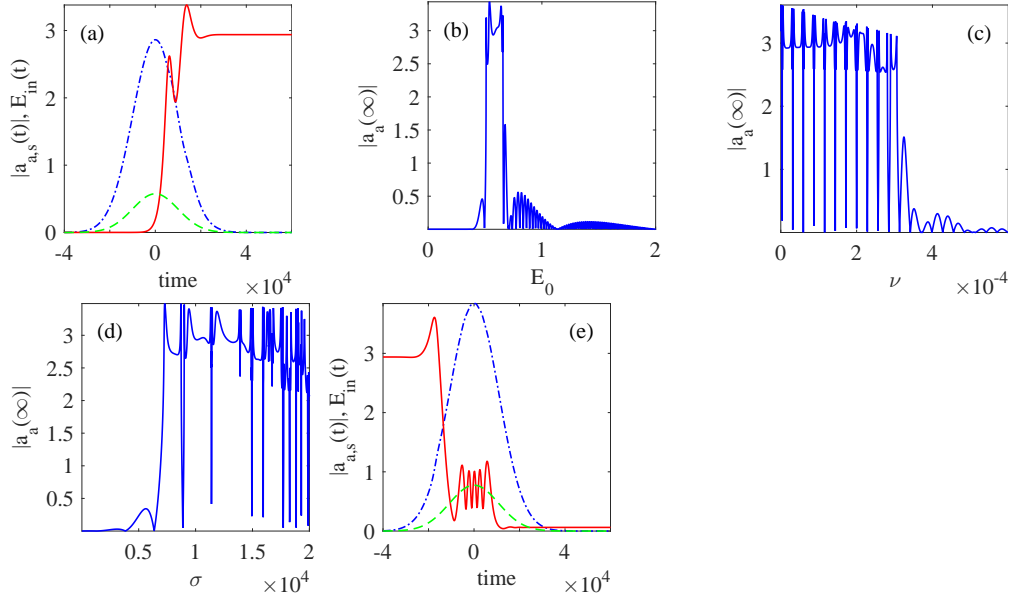

Fig. 2. (a). Amplitudes of eigenmodes of resonators under application of a gaussian pulse in the PhC waveguide shown in Fig. 1(a). Green dash line shows the profile of the injected pulse with parameters: $E_0 = 0.575, \nu = 10^{-4}, \sigma = 10000$, dash-dot line shows the symmetric mode amplitude $|a_s|$ and red solid line shows the amplitude of the antisymmetric $|a_a|$ BSC mode. The amplitude of trapped light $|a_a(\infty)|$ in the symmetry protected BSC vs: (b). Amplitude E_0, (c) The detuning parameter ν, and (d) The duration of impulse σ for $E_0 = 0.575$ of the gaussian pulse Eq. (6). (e). The release of light from BSC after application of a secondary gaussian pulse with $\sigma = 10797, \nu = 0.0001, E_0 = 0.7741$. The parameters of the resonators are the following: with the parameters $\omega_0 = 0.352, \gamma = 0.01, u = 0.001, \lambda = 0.0001$.

We rewrite Eq. (3) by use of $A_{s,a}(t) = a_{s,a}(t)e^{i\omega t}$ as follows

$$-i\dot{a}_s = (\nu + \lambda[|a_s|^2 + 2|a_a|^2])a_s + \lambda a_a^2 a_s^* + 2i\gamma a_s - i\sqrt{\gamma}E_{in}(t),$$
$$-i\dot{a}_a = (\nu + \lambda[|a_a|^2 + 2|a_s|^2])a_a + \lambda a_s^2 a_a^*. \tag{5}$$

where $\nu = \omega_0 - \omega$ is the detuning parameter. One can see from the above equations that although the antisymmetric mode a_a is decoupled from the injected light it can be excited via the nonlinear terms.

In order to trap light we apply a gaussian pulse of light

$$E_{in}(t) = E_0 \exp(-t^2/2\sigma^2). \tag{6}$$

Figure 2(a) shows that the injected gaussian pulse excites the symmetric mode a_s which follows the amplitude of the injected light pulse. When the symmetric mode is excited sufficiently it triggers excitation of the antisymmetric mode through the nonlinear terms in Eq. (5). After the pulse has passed by the resonator the symmetric mode leaks into the waveguide and the anti-symmetric mode becomes isolated from the waveguide, i.e., becomes a true BSC with trapped amplitude $|a_a(\infty)|$ as shown in Fig. 2(a). Figures 2(b) and 2(c) show that there are windows in the amplitude and frequency of gaussian pulse in which light storage takes place. The duration of gaussian pulse σ is to be of order $1/v$ or larger to result in high intensity of the captured light as shown in Fig. 2(d). Therefore the robust symmetric BSC is capable for light trapping, however the amount of storage energy proportional to $|a_a(\infty)|^2$ [35] is highly sensitive to the parameters of the injected gaussian pulse as seen from Figs. 2(b)-2(d). The application of the secondary pulse again opens the BSC according to Eq. (5) and the symmetry protected BSC leaks into the waveguide as shown in Fig. 2(e). The parameters of the secondary gaussian pulse $\sigma = 9885, E_0 = 0.7741, v = 0.0001$ give optimal effect of release. One can also see high dynamical response of the BSC mode when the secondary pulse is passed by [42].

3. Single microcavity

Miniaturization of photonic elements and efficient transport of light are two paramount issues required for the design of integrated photonic circuits. To address the above issues instead of two microresonators we use a single microresonator with two eigenmodes embedded into the propagation band of the waveguide. Then the localization occurs due to a full destructive interference of corresponding resonant modes [43]. Specifically, we exploit the design shown in Fig. 3(a) [25]. Four linear defect rods of the same radius but with dielectric constant ε different from the dielectric constant of host rods shown by green open circles are placed at the vertexes of a square. On the both sides of the resonator four additional rods are inserted in the waveguide in order to suppress the coupling of the resonator with the waveguide. Totally, these nine defect rods form a microresonator embedded into the PhC waveguide whose eigenfrequencies versus the dielectric constant ε are plotted in Fig. 3(b) together with the eigenmodes [41]. Note, both eigenmodes are symmetric relative to inversion of the y-axis shown in Fig. 3(a), and therefore are coupled with the symmetrical propagating mode in the waveguide channel. The eigenfrequencies of the monopole and quadrupole-diag modes cross while effect of other eigenmodes, two dipole and quadrupole-xy modes are not important [25] and are not shown in Fig. 3(b).

Assume, we can vary the dielectric constant ε of the defect rods. Then as shown in Fig. 3(b) the eigenfrequencies are crossing. It is important to note that both eigenmodes have the same parity as the parity of electromagnetic mode propagating over the waveguide. Therefore each mode would decay into the waveguide becoming a resonant mode with a finite resonant width. The reader can find specific values of the resonant widths in Ref. [25]. When the eigenfrequencies cross the resonances undergo avoiding crossing resulting in that one of the resonant widths turns to zero forming a BSC [25, 43]. Experimentally this scenario for BSC occurrence meets with difficulties of tuning the dielectric constant of defect rods that makes the BSC non robust [23, 25]. It is remarkable that the Kerr effect in the microresonator removes this difficulty. The robust BSC appears in a self-adaptive way due to the nonlinear shift of the dielectric constant [25, 31–33]. Therefore the design in Fig. 3 offers a capacity for light storage.

The temporary CMT equations for the relevant modes of the resonator take the following form with account of instantaneous Kerr effect

$$-i\dot{A}_1 = (\omega_1 + \lambda_{11}|A_1|^2 + i\gamma_1)A_1 + (u + \lambda_{12}(A_1A_2^* + A_1^*A_2) + i\sqrt{\gamma_1\gamma_2})A_2 - i\sqrt{\gamma_1}E_{in}(t),$$
$$-i\dot{A}_2 = (\omega_2 + \lambda_{22}|A_1|^2 + i\gamma_2)A_2 + (u + \lambda_{12}(A_1A_2^* + A_1^*A_2) + i\sqrt{\gamma_1\gamma_2})A_1 - i\sqrt{\gamma_2}E_{in}(t), \quad (7)$$

where the subscripts 1, 2 refer to the amplitudes of monopole and quadrupole-diag eigenmodes,
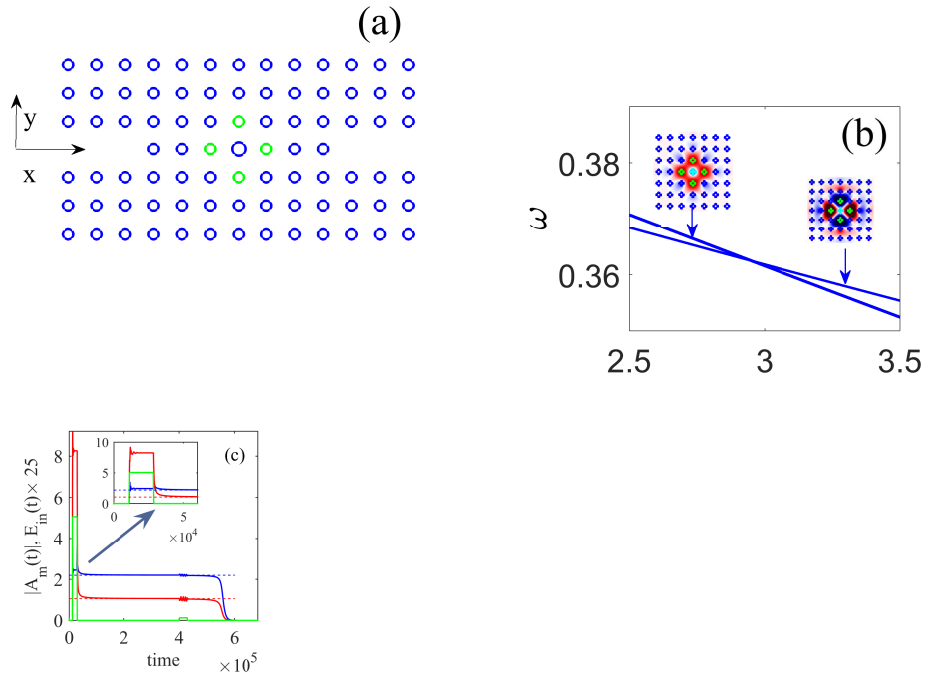
Fig. 3. (a). The same PhC structure as shown in Fig 1(a) however with single in-channel microresonator. Four linear defect rods of the same radius with dielectric constant ε are shown by green circles. (b). The eigenfrequencies of two eigenmodes (monopole and quadrupole-diag) shown as dependent on the dielectric constant of the central defect rod. (c). Light trapping by the BSC for the first pulse with amplitude $E_0 = 0.2$ and duration 2×10^4. The release of light by the secondary pulse with amplitude $E_0 = 0.006$ and duration 2×10^4. Inset shows details of excitation dynamics of eigenmode amplitudes after application of the first pulse. The parameters substituted into the CMT equations (9) are taken from Ref. [25]: $\omega_1 = 0.36, \omega_2 = 0.365, \gamma_1 = 3 \cdot 10^{-5}, \gamma_2 = 1.3 \cdot 10^{-4}, u = 1.77 \cdot 10^{-4}, \lambda_{11} = 10^{-4}$.

and nonlinear coefficients equal [35, 40]

$$\lambda_{mn} = \frac{\omega_0 n_0 c^2 n_2^2}{8\pi a^2} \int E_m^2(x,y) E_n^2(x,y) dx dy \qquad (8)$$

with normalization constants given by Eq. (4). The eigenmodes $E_m(x,y)$ are shown in Fig. 3(b). Integration includes host rods within a region of localization of the eigenmodes $E_m(x,y)$.

For the stationary process $E_{in}(t) = E_0 e^{i\omega t}, A_j(t) = A_j e^{i\omega t}$ the CMT equations (7) takes the following form

$$\begin{pmatrix} \omega_1 + \lambda_{11}|A_1|^2 - \omega + i\gamma_1 & u + \lambda_{12}(A_1 A_2^* + A_1^* A_2) + i\sqrt{\gamma_1 \gamma_2} \\ u + \lambda_{12}(A_1 A_2^* + A_1^* A_2) + i\sqrt{\gamma_1 \gamma_2} & \omega_2 + \lambda_{22}|A_2|^2 - \omega - i\gamma_2 \end{pmatrix} \begin{pmatrix} A_1 \\ A_2 \end{pmatrix} = -i \begin{pmatrix} \sqrt{\gamma_1} \\ \sqrt{\gamma_2} \end{pmatrix} E_0. \qquad (9)$$

The BSC occurs when the inverse of the matrix in Eq. (9) does not exist, i.e., when, the determinant of the matrix and respectively, one of the complex eigenvalues turns to zero. For the linear case formation of the BSC requires tuning of material parameters and occurs at [25]

$$\omega_2 - \omega_1 = \frac{u(\gamma_2 - \gamma_1)}{\sqrt{\gamma_1 \gamma_2}}, \omega_{BSC} = \omega_1 + u\sqrt{\frac{\gamma_2}{\gamma_1}}, \qquad (10)$$

For the nonlinear case Eq. (10) can be satisfied in a self-induced way [25, 31] without necessity to tune material parameters: $\omega_j \rightarrow \omega_j + \lambda_{jj}|A_j|^2, u \rightarrow u + \lambda_{12}(A_1 A_2^* + A_1^* A_2)$.

Two factors substantially weaken the nonlinear contribution of the quadrupole-diag mode. First, as seen from Fig. 3(a) two nodal lines of the quadrupole mode go through the central defect rod which enormously decreases the integrals in Eq. (8). Second, $\gamma_1 \ll \gamma_2$ that suppresses excitation of the quadrupole-diag mode amplitude A_2 compared to the monopole mode amplitude A_1. Therefore for simplicity we take $\lambda_{12} = 0, \lambda_{22} = 0$ and obtain from Eq. (10) that the BSC is achieved at fixed values of the mode intensities [25]

$$\lambda_{11}|A_{1c}|^2 = \omega_2 - \omega_1 + \frac{u(\gamma_2 - \gamma_1)}{\sqrt{\gamma_1 \gamma_2}}, |A_{2c}|^2 = \frac{\gamma_1}{\gamma_2}|A_{1c}|^2 \qquad (11)$$

when the intensities of monopole and quadrupole-diag modes become equal, respectively,

$$I_{2c} = |A_{2c}|^2 = \frac{\gamma_1}{\gamma_2} I_{1c}, I_{1c} \ll I_{2c}, \quad \omega_{BSC} \approx \omega_2 - u\sqrt{\frac{\gamma_1}{\gamma_2}}. \qquad (12)$$

Thus the amplitudes A_m of the BSC eigenmode are fixed and depend only on the design of the optical microresonator and material parameters. Therefore, the amount of trapped light by the BSC is also fixed. The amount does not depend on the basic frequency and profile of a light pulse. Therefore for successful light storage the amount of pulse power should be enough to populate the BSC with the intensity given by Eqs. (11) and (12). The process of trapping numerically computed and shown in Fig. 3(c) agrees with this consideration. One can see that at first both mode amplitudes $A_m, m = 1, 2$ follow the pulse. After the time of order 10^4 the amplitudes stick to the BSC amplitudes given by Eq. (11) shown by dash lines in Fig. 3(c). The light accumulated in the resonator remains trapped until the next gaussian pulse is applied.

4. Fabry-Perot BSC

The next design is close to that considered in section 2, however two defect nonlinear rods are positioned at some distance L between each other as shown in Fig. 4(a). Each defect rods presents off-channel nonlinear microresonator which gives rise to a full reflection at the frequency dependent on the intensity of light [44]. Therefore these two off-channel resonators
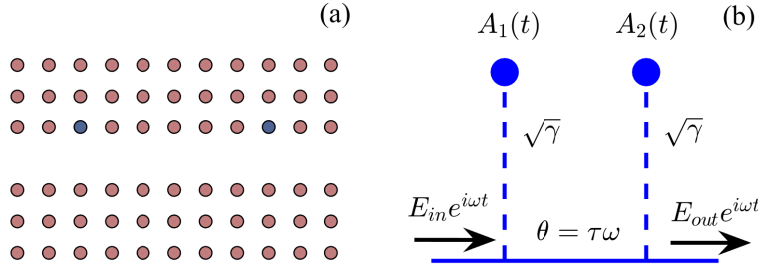
Fig. 4. (a). Layout of 2D PhC which forms the Fabry-Perot resonator. Two defect rods shown by gray with the Kerr effect are inserted near by PhC waveguide. (b). Equivalent CMT presentation for PhC layout with equivalent parameters: $\gamma = 0.01, \lambda = 0.0001, \omega_0 = 0.352, u = 0$.

form a Fabry-Perot resonator. Then if the distance between the microresonators is tuned to fulfill the integer half-wavelength condition [32] the system supports a BSC. For simplicity we consider that only defect rods shown by gray in Fig. 4(a) are subjected to the Kerr effect and neglect the nonlinear phase shift in the waveguide. The CMT equations have the following form [13, 45]

$$-i\dot{A}_1 = (\omega_0 + \lambda |A_1|^2 + i\gamma)A_1 + i\gamma A_2 e^{i\theta} - i\sqrt{\gamma}E_{in}(t)e^{i\omega t},$$
$$-i\dot{A}_2 = (\omega_0 + \lambda |A_2|^2 + i\gamma)A_2 + i\gamma A_1 e^{i\theta} - i\sqrt{\gamma}E_{in}(t)e^{i\omega t + i\theta}, \qquad (13)$$

where θ is the phase shift incurred as the wave travels from the first defect to the second one. For a monochromatic wave $\theta = k(\omega)L$. However for a light pulse which is an expansion over monochromatic waves these equations (13) are not valid. Therefore we have to modify Eq. (13) taking into consideration the delay time τ for travelling from one microcavity to another:

$$-i\dot{A}_1 = (\omega_0 + \lambda |A_1|^2 + i\gamma)A_1 + i\gamma A_2(t - \tau) - i\sqrt{\gamma}E_{in}(t)e^{i\omega t},$$
$$-i\dot{A}_2 = (\omega_0 + \lambda |A_2|^2 + i\gamma)A_2 + i\gamma A_1(t - \tau) - i\sqrt{\gamma}E_{in}(t - \tau)e^{i\omega(t - \tau)}. \qquad (14)$$

For stationary process with $a_j(t) = A_j e^{i\omega t}$, $\theta = \tau\omega$. Equation (14) can be obtained from Eq. (13) after the substitution ω with the differential operator $i\frac{\partial}{\partial t}$. Then we have $A_j(t - \tau) = \exp[i\tau\frac{\partial}{\partial t}]A_j(t) = \exp(i\theta)A_j(t)$. The BSC occurs if the determinant of the matrix in the stationary CMT equations

$$\begin{pmatrix} \omega_0 + \lambda |A_1|^2 - \omega + i\gamma & i\gamma e^{i\tau\omega} \\ i\gamma e^{i\tau\omega} & \omega_0 + \lambda |A_2|^2 - \omega + i\gamma \end{pmatrix}$$

equals zero [32]. That condition gives us

$$\tau\omega = \pi n, \ |A_{1c}|^2 = |A_{2c}|^2 = \frac{1}{\lambda}\left(\frac{\pi n}{\tau} - \omega_0\right), \qquad (15)$$

where n is an integer. For the parameters listed in Fig. 4 and $\omega = \omega_0 + v, \tau = \pi/\omega$ we obtain the amplitudes of the intensities of the BSC take discrete value defined by the ratio $\frac{v}{\lambda}$ for

$n = 1$. They are are shown in Fig. 5(a) by black dash lines. The numerical solution of Eq. (14) shows as injected gaussian pulse is captured at this BSC as shown in Fig. 5(a) provided that the amplitude of the injected pulse exceeds the threshold similar to the previous design with single microresonator. Application of the secondary pulse releases captured light. In Fig. 5(b) we present the most optimal process which occurs at the parameters of the gaussian pulse listed in figure caption. As different from the case of single microresonator in section 3, the BSC intensities are discretized by integer n as given by Eq. (15). Therefore application of larger pulse intensities can give rise to trapping of light in the next BSCs with $n > 1$.
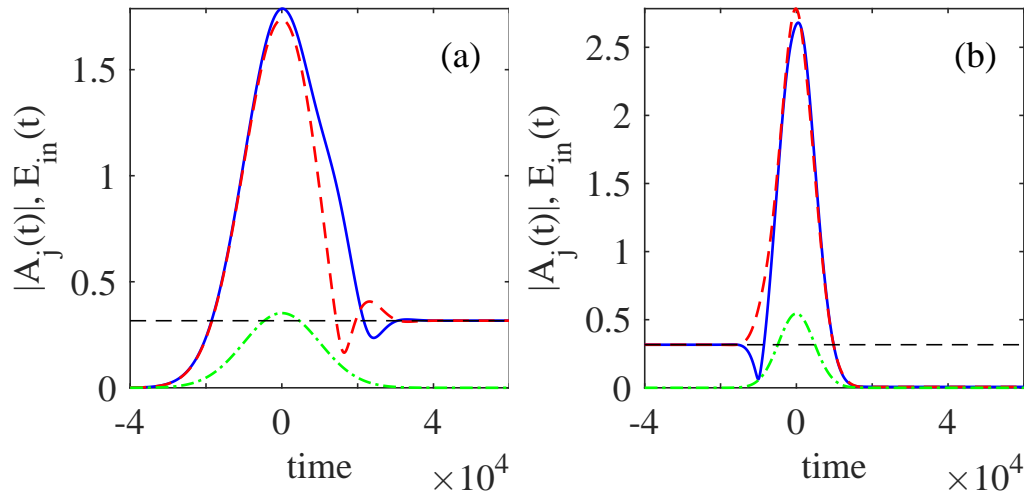

Fig. 5. Time evolution of mode amplitudes $|A_1|$ (blue solid line) and $|A_2|$ (red dash line) after the injection of a first gaussian pulse shown by green dash-dot line with $\sigma = 10000, E_0 = 0.3522, v = 10^{-5}$ (a) and a secondary pulse with $\sigma = 4705, E_0 = 0.545, v = 10^{-5}$. Black dash lines show the BSC amplitude given by Eq. (15).

5. Discussion and conclusions

In regard to stability the approaches based on stopping light in linear PhC designs briefly discussed in the Introduction are preferable compared to the light storage in BSCs in nonlinear PhC structures. Moreover the linear system can operate at any light intensity while the light storage in the self-induced BSCs is possible only if the amplitude of the injected pulse exceeds a certain threshold sufficient to populate discrete value of the BSC intensity . The process of light slowing demands tuning of operational frequency of light to the specific points of the frequency spectrum of waveguide where the group velocity of light tends to zero. While the only requirement in the present approach is that the BSC frequencies reside in the propagation band of PhC waveguide. The next fundamental advantage of the BSC designs is a ultra-high compactness. The trapping of light in a single defect rod due to a full destructive interference of the monopole and quadrupole-diag modes [43] occurs in the volume of order of $a^2 h$ where a is the period of 2D PhC and h is the length of the rods. While the former linear designs for light storage require much more volume. The second advantage of exploiting the self-induced BSC is that the light can be easily released by a secondary pulse rendering the process of storage and release by demand all-optical. Instead of the Kerr effect resulting in self-induced BSCs we can utilize a local heating or local deformation of the PhC to reach the condition for the BSC in controllable manner. However these approaches deprive the advantage of all-optical

manipulation.

In the present paper we considered the phenomenon of light storage and release by the bound states in the continuum in the framework of temporal coupled mode theory with the parameters borrowed from numerical calculations for real 2D PhC structures. Direct study of these processes in PhC designs requires extremely time consuming computations even for the case when the nonlinearity is accounted for only the defect rods. The temporal CMT allows us easily asses merits and disadvantages of the PhC designs considered in sections 2-4. The first design consists of a waveguide with two off-channel nonlinear microresonators weakly coupled with the waveguide. The design holds the antisymmetric mode shown in Fig. 1(c) which is decoupled from the symmetric propagating mode and thereby is determined as a symmetry protected bound state. Application of a light pulse damages this BSC as the pulse passes by the microresonators because of nonlinear interaction of the BSC with the symmetrical mode as seen from Eq. (5). As the result some amount of light is trapped in the BSC after the pulse has been passed. However the next pulse is again coupled with the BSC giving rise to release of captured light. Figures 2(b)–2(d) show that the light storage is highly sensitive to the parameters of the gaussian pulse. That is result of the BSC intensity or equivalently the BSC frequency depends on to which extend the BSC is populated.

In the next section we considered different PhC design with a single in-channel microresonator in which the BSC is a result of full destructive interference of two resonant modes. In the linear case the occurrence of BSC would require tuning of the material parameters. It is remarkable that due to the Kerr effect BSCs occur by self-induced way as it was shown in Refs. [25, 31, 33] if the intensity of accumulated light achieves critical values given by Eq. (12). Finally we considered in the framework of the temporal CMT the Fabry-Perot PhC structure shown in Fig. 4. The temporal CMT equations were modified to account for the delay times to yield Eq. (14). This design also supports self-induced BSCs as was shown in Ref. [32] however with multiple discretized BSC intensities as given by Eq. (15). That gives more freedom in light storage compared to the previous design.

There are processes of irreversible light emission due to finite thickness of 2D PhC as well as due to imperfectness of the structure which take place for any approach. That will restrict the storage in time. Also the nonlinear resonator has a risk of bifurcation into modes coupled with different waveguide channels or radiation modes for example because of modulation instability of enough long nonlinear defect rod. These processes can be readily involved into the CMT approach by expansion of number of modes of the microresonator and number of channels coupled with the modes. But it is clear that a criteria to exclude these unwanted modes is the frequency distance between useful modes and unwanted modes should substantially exceed the perturbation due to the Kerr effect. In the present paper we consider this criteria is fulfilled.

Let us estimate the values of the power of injected light which are necessary to achieve the all-optical storage and release by demand. The nonlinearity constant is estimated in order of magnitude as 10^{-4}. Then the injected amplitude in terms of CMT equations $E_0 = 1$ corresponds to $625W/a$ where $a = 0.5\mu m$ is the lattice unit. Therefore in order to store light in the symmetry protected BSC (section 2) by gaussian pulse its power should exceed $E_0^2 \cdot 625W/a$. For the length of rods compared to a we obtain that power injected into the waveguide channel should be around 180 W. However this power can be reduced further when the tuning parameter v is decreased as it is seen from Fig. 2(b). Similar estimates can be applied for other PhC designs in Sections 3 and 4. However these designs demand that the injected amplitude exceed the threshold values. For the single microresonator in section 3 the injected power should exceed $25W$. For the Fabry-Perot design we obtain the value around 100 W however this power also can be reduced with decereasing of the tuning parameter v. It is very important to notice the Kerr effect is small $\lambda \sim 10^{-4}$. Therefore to compensate for small λ we have to tune v to be the

same order in magnitude as λ. The same refers to the duration of the gaussian pulse σ which has to be of order $1/\nu$.

5.1. Acknowledgments